NANO LETTERS

pubs.acs.org/NanoLett Letter

DNA Delivery by Virus-Like Nanocarriers in Plant Cells

Md Reyazul Islam,[#] Marina Anderson-Youngblood,[#] Hye-In Kim, Ivonne González-Gamboa, Andrea Gabriela Monroy-Borrego, Adam A. Caparco, Gregory V. Lowry, Nicole F. Steinmetz,* and Juan Pablo Giraldo*

Cite This: https://doi.org/10.1021/acs.nanolett.3c04735 Read Online

ACCESS | Metrics & More | Article Recommendations | Supporting Information

ABSTRACT: Tobacco mild green mosaic virus (TMGMV)-like nanocarriers were designed for gene delivery to plant cells. High aspect ratio TMGMVs were coated with a polycationic biopolymer, poly(allylamine) hydrochloride (PAH), to generate highly charged nanomaterials (TMGMV-PAH; 56.20 ± 4.7 mV) that efficiently load (1:6 TMGMV:DNA mass ratio) and deliver single-stranded and plasmid DNA to plant cells. The TMGMV-PAH were taken up through energy-independent mechanisms in *Arabidopsis* protoplasts. TMGMV-PAH delivered a plasmid DNA encoding a green fluorescent protein (GFP) to the protoplast nucleus (70% viability), as evidenced by GFP expression using confocal microscopy and Western blot analysis. TMGMV-PAH were inactivated (iTMGMV-PAH) using UV cross-linking to prevent systemic infection in intact plants. Inactivated iTMGMV-PAH-mediated pDNA delivery and gene expression of GFP *in vivo* was determined using confocal microscopy and RT-qPCR. Virus-like nanocarrier-mediated gene delivery can act as a facile and biocompatible tool for advancing genetic engineering in plants.

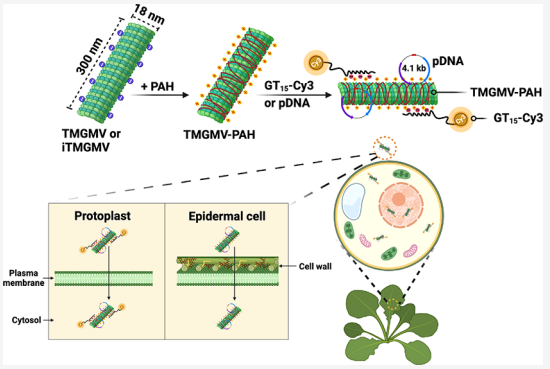

KEYWORDS: *virus, nanoparticles, gene delivery, protoplasts, plant genetics, agriculture*

The rapid increase in the human global population is projected to require a 35 to 55% increase in food production by 2050.[1] Addressing this challenge during a changing climate and without sustainable conventional agricultural practices raises concerns about food security.[2] Plant genetic engineering has been widely employed to generate crops with increased yield,[3] improved quality, enhanced resistance to herbicides,[4] insects,[5] diseases,[6,7] and biotic and abiotic stresses.[8,9] Genetically modified plants for biomanufacturing also hold immense potential for synthesizing small-molecule drugs,[10] recombinant protein therapeutics,[11,12] and vaccines.[13,14] Despite numerous biotechnological advancements over the past few decades, the genetic transformation of many plant species still poses considerable challenges. The delivery of transgenes into plant species mainly relies on two transformation methods: *Agrobacterium tumefaciens*-mediated transformation system[15] and particle bombardment.[16] However, the *Agrobacterium*-mediated system has some significant drawbacks such as uncontrollable target gene integration into the host chromosomes causing positional effects on gene expression, and many plant species are inherently resistant to *Agrobacterium* infection[17] or showed low transformation efficiency (~5% to 33%).[18,19] Biolistics has been utilized in various plant species, as a random gene delivery system into the host nucleus, mitochondria, and chloroplast.[4] Particle bombardment is performed by high-pressure gene gun delivery that damages host genomic DNA and results in random insertions of multiple copies of the gene[20] The particle bombardment system is also expensive, requires labor-intensive tissue culture and selection, has low transformation efficiency often requiring hundreds of transformation attempts to generate a transgenic line,[20,21] and has not been successfully implemented in diverse plant species.[22] Therefore, there is a pressing need for a versatile, plant-species-independent, and easy-to-use tool for plant genetic transformation, allowing for efficient delivery of exogenous genes.

Recent advancements in nanotechnology have revealed the potential of nanomaterials in facilitating the delivery of genetic materials, such as plasmid DNA[23−25] and siRNA,[26,27] as well as biomacromolecules like functional proteins,[28] active ingredients,[29,30] nutrients,[31] and therapeutics[32] in plants. Single-walled carbon nanotubes (SWCNTs),[23,24,33] mesoporous silica nanoparticles (MSNs),[34,35] layered double hydroxide (LDH) clay nanosheets,[26] and functional peptide−DNA complexes[25,36] have demonstrated delivery of functional DNA/RNA cargoes into plant cells without mechanical assistance.

Received: December 4, 2023
Revised: June 10, 2024
Accepted: June 12, 2024

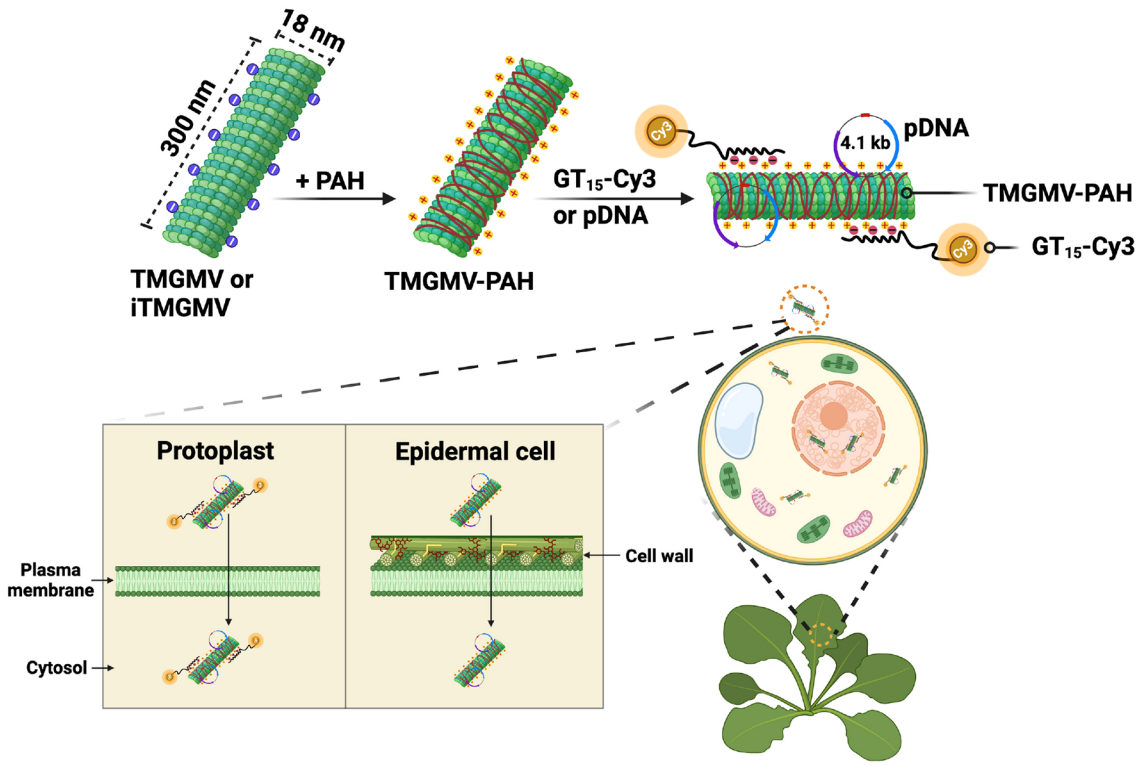

Figure 1. Intracellular DNA delivery in *Arabidopsis* plant cells mediated by virus-like nanocarriers. Negatively charged TMGMVs or inactivated (iTMGMVs) were coated with a biopolymer, poly(allylamine) hydrochloride (PAH), imparting them with positive charge (TMGMV-PAH). The TMGMV-PAH were loaded by electrostatics with a DNA oligo (GT_{15}, 30 bp ssDNA) that was covalently linked to a Cy3 organic dye (TMGMV-PAH-GT_{15}-Cy3), or a plasmid DNA (pDNA) encoding a reporter gene of a green fluorescent protein (GFP). The nanocarriers and DNA cargoes spontaneously enter plant cell membranes without mechanical aid through energy-independent uptake mechanisms. Inactivated iTMGMV-PAH mediated the delivery and expression of pDNA in *Arabidopsis* epidermal cells.

Several studies have demonstrated the possibility of carbon nanotube-mediated gene delivery in plant nucleus,[23,36] chloroplast,[24,33] and mitochondrial[25] genomes. However, there is a need to develop high aspect ratio nanomaterials for plant transformation that are degradable, biocompatible, and manufactured with controlled aspect ratios on a large scale. We turned toward plant virus nanoparticles as a biodegradable, cost-effective, and easily scalable nanotechnology with tunable surface chemistry.[29,30,37]

Tobacco mild green mosaic virus (TMGMV)[38] is a plant virus within the tobamovirus genus, also known as the U2 strain of tobacco mosaic virus (TMV), approved by the U.S. Environmental Protection Agency (EPA) for use in bio-herbicides.[39] The nucleoprotein components of TMGMV are self-assembled from 2130 identical copies of a coat protein and ssRNA to form a 300 × 18 nm soft matter rod-shaped structure with a 4 nm wide hollow interior channel.[29,38,40] The nanocarriers derived from TMGMV are of interest for delivery applications due to their unique physio-chemical properties, such as biodegradability (protein-based particles), the ability to self-assemble into identical and high aspect ratio structures, and large-scale economical production with high purity and reproducibly.[29,41] The chemical design space is well understood and TMGMV can be functionalized with cargo through covalent chemistry[42] or encapsulation.[29] There are also well-established methods of TMGMV RNA inactivation through UV cross-linking or chemical treatments for use in plant species susceptible to infection.[43] TMGMV particles have been utilized as a carrier for active ingredients such as a porphyrin-based photosensitizer drugs (500 Zn-porphyrin molecules/TMGMV) for cancer cell abolition of melanoma and cervical cancer models,[40] as well as ivermectin (10% mass loading efficiency to TMGMV) to treat plants infected with parasitic nematodes.[29,30,44] Plant virus-derived vectors (plasmids with virus genetic elements) have been extensively used for genetic engineering in plants through the mechanical inoculation of plasmid DNA, biolistics, vascular puncture, agroinoculation, or insect-mediated vector delivery.[45,46] These applications focused on delivery of RNA packaged inside the capsid.[47] To date, plant virus coat proteins have not been engineered as carriers for facile plasmid DNA delivery in plant cells.

In this study, we developed native and inactivated TMGMV-based nanomaterials as a platform for the nuclear delivery of DNA in *Arabidopsis thaliana* protoplasts and intact plants, respectively (Figure 1). Although PEG-mediated protoplast transformations achieve high transient transformation efficiencies (50−90% in viable cells),[48] protoplast systems are crucial for developing genetic transformation tools and understanding nanoparticle−plant cell interaction processes.[23,33,49] Because plant protoplasts lack a cell wall, this study also included DNA delivery analysis *in vivo* using *Arabidopsis* leaf epidermal cells. We functionalized TMGMV by covalently coating a poly-cationic biopolymer, poly(allylamine) hydrochloride (PAH), on the TMGMV surface (TMGMV-PAH). The PAH imparts a positive charge to TMGMV-PAH for binding to DNA through electrostatic interactions. PAH has been extensively used for pharmaceutical and drug delivery applications due to its high water-solubility and biodegradable properties.[50,51] To determine whether TMGMV-PAH delivered single-stranded DNA (ssDNA) into protoplast cells without using mechanical aid

https://doi.org/10.1021/acs.nanolett.3c04735
Nano Lett. XXXX, XXX, XXX−XXX

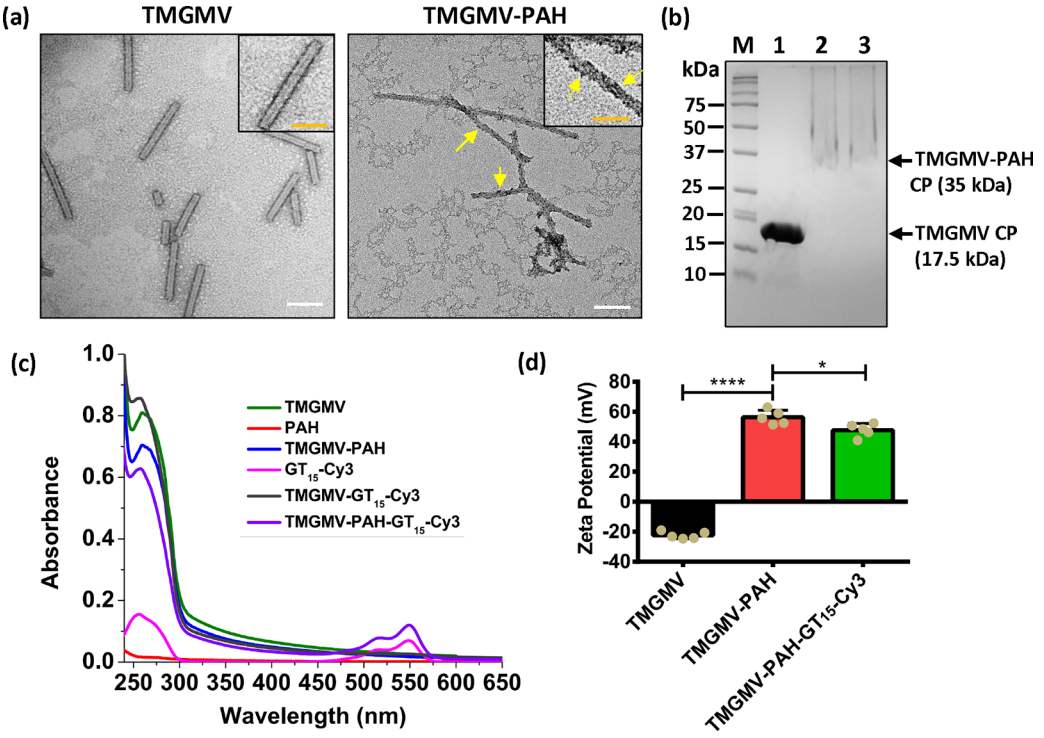

Figure 2. Characterization of TMGMV-PAH coated with single-stranded DNA. (a) Transmission electron microscopy of negative-stained TMGMV and TMGMV-PAH. Yellow arrows indicate PAH coated on the surface of TMGMV. Scale bars 100 nm. (b) Denaturing Nu-PAGE gel electrophoresis under white light followed by Coomassie staining, 1: TMGMV, 2: TMGMV-PAH, 3: TMGMV-PAH-GT_{15}-Cy3, M: prestained molecular weight standards. The arrow indicates the position of the TMGMV coat protein (CP) at 17.5 kDa (lower arrow) and PAH conjugated TMGMV-PAH CP at 35 kDa (upper arrow) or higher molecular weight. (c) UV−vis absorbance and (d) zeta potential (10 mM MES, pH 6.0) of TMGMV before and after coating with PAH and GT_{15}-Cy3. The data are the means ± SD (n = 4). Statistical analysis was performed by one-way analysis of variance (ANOVA) with Tukey's *posthoc* multiple comparison analysis (GraphPad Prism 6); *P < 0.05; ****P < 0.0001.

while maintaining biocompatibility, we employed confocal microscopy to track the ssDNA cargo covalently bonded to a fluorophore (Cy3) and protoplast bioavailability assays. We also demonstrated the high loading capacity of plasmid DNA (pDNA) onto the TMGMV-PAH, and assessed the pDNA delivery, uptake mechanism, and transgene expression in protoplasts. Finally, we used inactivated iTMGMV-PAH to demonstrate pDNA delivery and expression in *Arabidopsis* leaf epidermal cells *in vivo*. Using virus-like nanocarriers for DNA delivery in plant cells offers a promising solution for plant genetic transformations that is scalable and biocompatible with high manufacturing quality and reproducibility.

The selection of polymer coating for TMGMV focused on cationic biopolymers capable of binding electrostatically with negatively charged pDNA. Among various options, PAH, polylysine, and polyarginine were prioritized due to their higher pK_a values (above pH 8) and FDA approval for other applications. TMGMV coated with polylysine and polyarginine were negatively charged, making them unsuitable for pDNA coating (Figure S1). In contrast, PAH TMGMVs were positively charged, and therefore, PAH was chosen as the coating for TMGMV in this study. We characterized TMGMV, TMGMV-PAH, and GT_{15}-Cy3-loaded TMGMV-PAH (TMGMV-PAH-GT_{15}-Cy3) by UV−vis, dynamic light scattering (DLS), zeta potential (ζ), transmission electron microscopy (TEM), Nu-PAGE protein analysis, and fluorescence emission spectra. TEM imaging of TMGMV and TMGMV-PAH shows high aspect ratio, rod-shaped nanostructures (Figure 2a) consistent with previous studies using TMGMV for pesticide delivery.[29,42] The TMGMV-PAH had a rough surface, which is different from native TMGMV (Figure 2a), indicating coating of the PAH polymer on the TMGMV surface. We utilized a carbodiimide coupling reaction to covalently bond the amine functional groups of PAH to the carboxyl groups in TMGMV (Figure S2),[42] and the chemical conjugation was confirmed by Fourier-transform infrared spectroscopy (FTIR; Figure S3). Based on TEM analysis, the average lengths of TMGMV and TMGMV-PAH were nonsignificantly different, 129.9 ± 57.7 and 191.3 ± 95 nm, respectively. Notably, broken nanomaterials were also observed in both uncoated TMGMV and TMGMV-PAH, which can occur during preparation or imaging of the TMGMV TEM samples.[29,42] Furthermore, the conjugation of PAH (~17.5 kDa) to TMGMV coat protein (CP) was confirmed by denatured Nu-PAGE protein analysis, which indicated the presence of higher molecular weight bands at ~35 kDa, in addition to the TMGMV CP band at ~17.5 kDa (Figure 2b). The smeared protein bands were observed due to the high positive charge of TMGMV-PAH CP (56.20 ± 4.7 mV) that hinders the relative mobility toward the electrode in the Nu-PAGE system. Both TEM and Nu-PAGE analysis indicate that PAH is coated onto the TMGMV-PAH.

To investigate DNA delivery by TMGMV-PAH in protoplasts, we used confocal microscopy to track ssDNA oligonucleotide $(GT)_{15}$ covalently linked to the Cy3 fluorescent dye (GT_{15}-Cy3). Cy3 is bright, photostable, and its emission range does not overlap with chloroplast autofluorescence.[24] GT_{15}-Cy3 has been previously employed for coating positively charged carbon nanotubes for determining subcellular localization in plants.[24,33,52] The UV−vis

https://doi.org/10.1021/acs.nanolett.3c04735
Nano Lett. XXXX, XXX, XXX−XXX

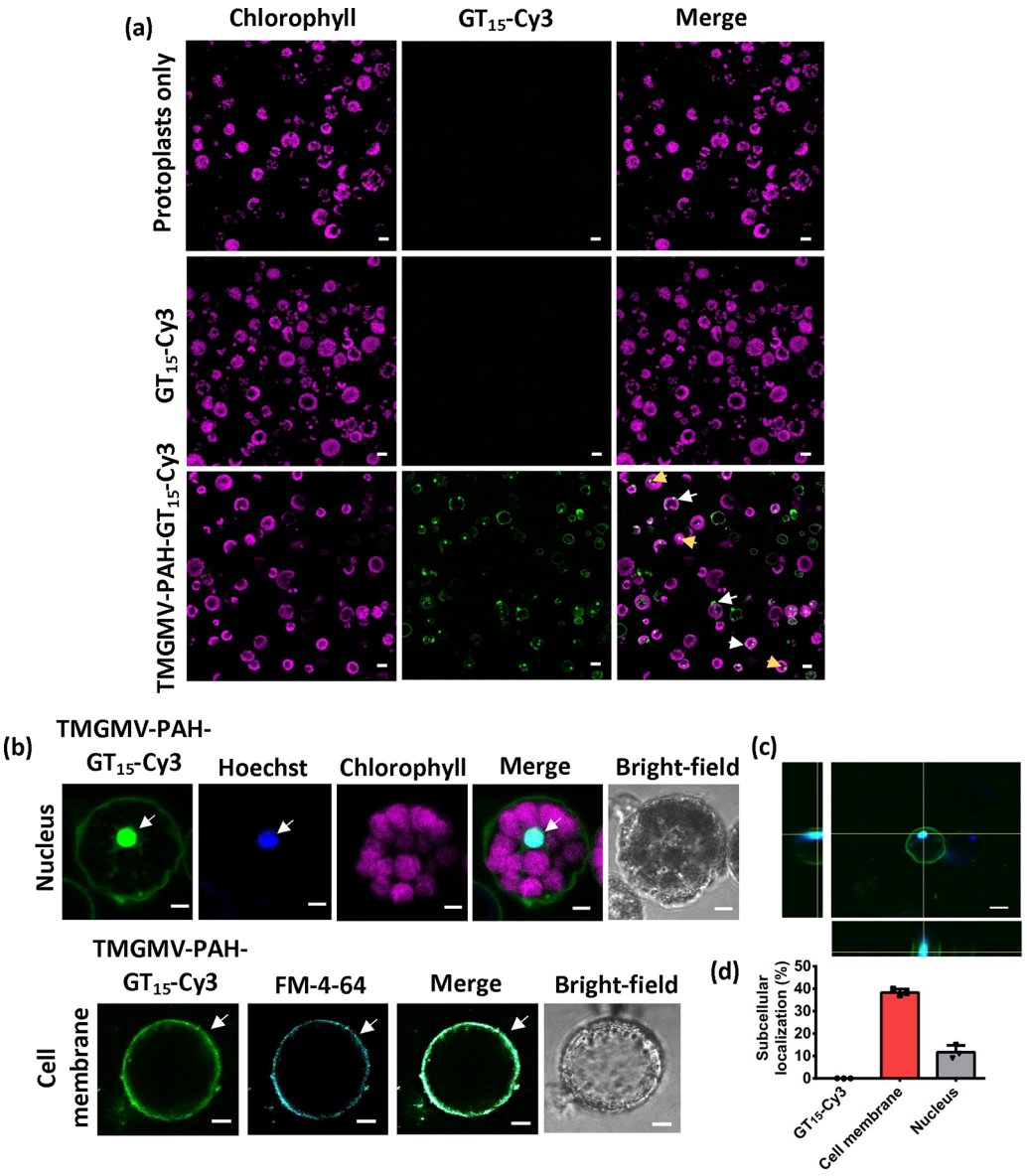

Figure 3. Delivery of single-stranded DNA by TMGMV-PAH in plant protoplasts. (a) Confocal images of isolated mesophyll protoplasts with chlorophyll autofluorescence (magenta) exposed to TMGMV-PAH-GT_{15}-Cy3 (0.1 mg/mL). The GT_{15}-Cy3 was detected in protoplast membranes (white arrows) and nuclei (yellow arrows). Scale bars 30 μm. (b) After treatment with TMGMV-PAH-GT_{15}-Cy3, protoplasts were stained either with a nuclear marker, Hoechst, or cell membrane staining dye, FM-4-64 for confocal microscopy imaging. Scale bars 5 μm. (c) Orthogonal projections from z-stacks of different planes (x/y, x/z, or y/z) of confocal microscopy images indicating localization of GT_{15}-Cy3 with Hoechst nuclear marker. Scale bars 30 μm. (d) Quantitative analysis of subcellular localization of GT_{15}-Cy3 with Hoechst nuclear marker and FM-4-64 cell membrane dye. The data are means ± SD (n = 3).

absorbance spectra of TMGMV, TMGMV-PAH, and TMGMV-PAH-GT_{15}-Cy3 indicated characteristic absorption peaks at 260 nm (Figure 2c). TMGMV-PAH-GT_{15}-Cy3 showed distinct absorption peaks at 550 nm that corresponded to the Cy3 dye on TMGMV-PAH (Figure 2c). To validate the binding of GT_{15}-Cy3 to TMGMV-PAH and confirm the absence of unbound dye, the sample was purified using a centrifugal filter unit (100 K MWCO). Following the second wash step, no absorbance corresponding to GT_{15}-Cy3 was detected in the eluent (Figure S4a), whereas TMGMV-PAH-GT_{15}-Cy3 exhibited fluorescence emission peaks at 567 nm, attributed to the attachment of GT_{15}-Cy3 on TMGMV-PAH (Figure S4b). DLS analysis indicated well dispersed nanomaterials with increasing hydrodynamic diameter from 267 ± 1.6 nm for TMGMV to 310 ± 1.3 nm for TMGMV-PAH and 361 ± 3.2 nm for TMGMV-PAH-GT_{15}-Cy3 (P < 0.005; Figure S4c). We observed a significant change of ζ potential after conjugation of PAH from negative charged TMGMV (−22.37 ± 2.3 mV) to highly positive charged TMGMV-PAH (56.20 ± 4.7 mV; P < 0.0001; 10 mM MES buffer, pH 6.0; Figure 2d), indicating binding of polycationic PAH to the TMGMV surface. As expected, the ζ potential for TMGMV-PAH slightly decreased from 56.20 ± 4.7 to 47.69 ± 4.4 mV when loading GT_{15}-Cy3 (P < 0.05; Figure 2d) due to the electrostatic bonding between the negatively charged GT_{15} and the positively charged TMGMV-PAH.

To examine *in vitro* DNA delivery and subcellular localization in plant cells using TMGMV-PAH as a nanocarrier, *Arabidopsis* protoplasts were isolated and incubated with TMGMV-PAH coated with GT_{15}-Cy3. Protoplasts are model

https://doi.org/10.1021/acs.nanolett.3c04735
Nano Lett. XXXX, XXX, XXX−XXX

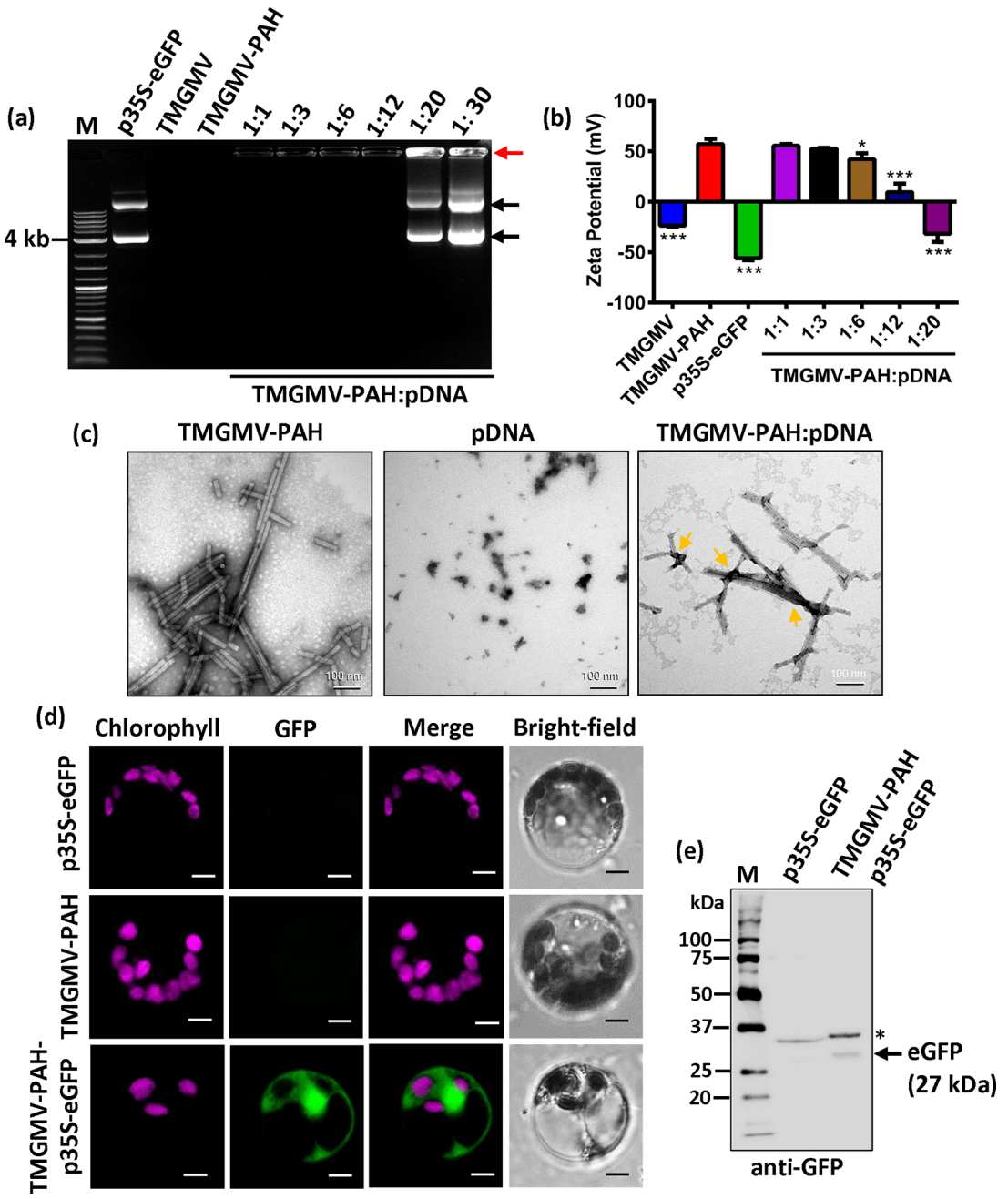

Figure 4. Plasmid DNA delivery and expression mediated by virus-like nanocarriers in isolated plant protoplasts. (a) DNA loading analysis by agarose gel electrophoresis of pDNA (p35S-eGFP) bound to TMGMV-PAH at mass ratios 1:1 to 1:30. M: DNA ladder. Black arrows indicate supercoiled (below) and circular (upper) pDNA bands. The red arrow indicates pDNA bound to TMGMV-PAH that prevents its mobility through the gel. (b) Zeta potential measurements of virus-like nanocarriers with or without pDNA (10 mM MES, pH 6.0). Data are means ± SD (n = 3–4). Statistical analysis was performed by one-way ANOVA and *Dunnett's* multiple comparisons posthoc test; *P < 0.01; ***P < 0.0001. (c) Representative TEM images of TMGMV, TMGMV-PAH, and pDNA-loaded at 1:6 mass ratios to TMGMV-PAH. Scale bar 100 nm. Arrows indicate pDNA attachment to TMGMV-PAH. (d) pDNA delivery and expression mediated by TMGMV-PAH in isolated plant protoplasts determined by confocal microscopy. Scale bar 10 μm. (e) GFP expression analysis by Western blotting. The arrow indicates 27 kDa of GFP protein and asterisks indicate nonspecific bands. M, protein ladder.

systems for gene expression analysis that have been used in numerous plant nanoparticle studies of uptake and gene delivery.[23,33,49] To assess the delivery of GT_{15}-Cy3 bound to TMGMV-PAH and their subcellular localization using confocal microscopy, isolated protoplasts (Figure S5) were incubated with 0.1 mg/mL of TMGMV-PAH-GT_{15}-Cy3 at room temperature for 2 h before imaging. Confocal fluorescence microscopy images indicated a significant level of GT_{15}-Cy3 fluorescence signal in protoplast cell membranes, and nuclei when treated with TMGMV-PAH-GT_{15}-Cy3 (Figure 3a). In contrast, control confocal images of protoplasts treated with GT_{15}-Cy3 did not show GT_{15}-Cy3 fluorescence signal indicating that GT_{15}-Cy3 alone cannot be taken up by protoplasts under these exposure conditions (Figure 3a). To confirm TMGMV-PAH-GT_{15}-Cy3 interaction with protoplast cell membranes and GT_{15}-Cy3 nuclear delivery by TMGMV-

https://doi.org/10.1021/acs.nanolett.3c04735
Nano Lett. XXXX, XXX, XXX−XXX

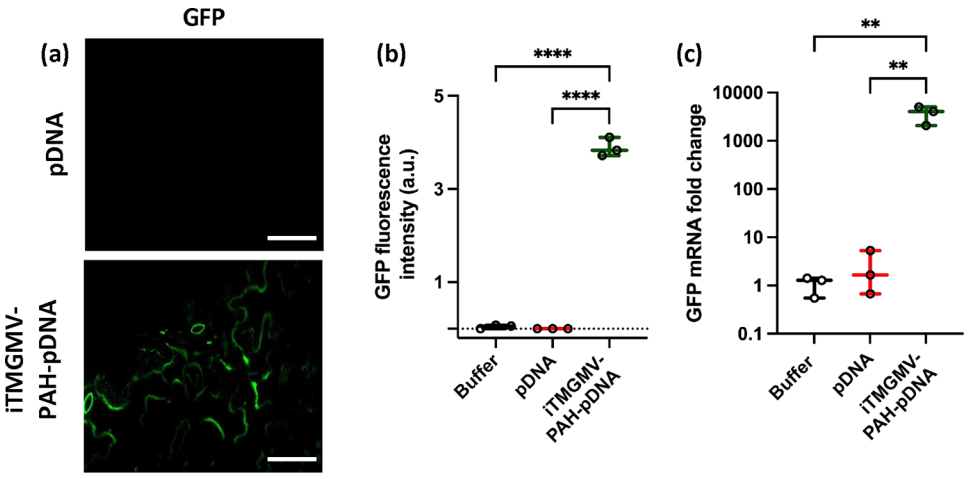

Figure 5. Plasmid DNA delivery and expression mediated by iTMGMV-PAH-pDNA in *Arabidopsis* leaves. Green fluorescence protein (GFP) (a) confocal microscopy images and (b) and fluorescence intensity ($n = 3$) indicating GFP expression in leaf epidermal cells infiltrated with iTMGMV-PAH-pDNA. Three-week-old *Arabidopsis* leaves were abaxially infiltrated with (1:6) 0.1 mg/mL iTMGMV-PAH: 0.6 mg/mL pDNA and analyzed 2 days post infiltration ($n = 3$). Scale bars 30 μm. One-way ANOVA with Tukey's *posthoc* multiple comparison analysis; ****$P < 0.0001$. (c) RT-qPCR analysis of GFP mRNA expression levels after 2 days of iTMGMV-PAH-pDNA infiltration in *Arabidopsis* leaves. Statistical analysis was performed by one-way ANOVA with Tukey's *posthoc* multiple comparison analysis; **$P < 0.005$ ($n = 3$).

PAH, protoplasts were stained with a cell membrane marker FM-4-64 and a nuclear staining marker Hoechst. The GT_{15}-Cy3 fluorescence was observed localized with FM-4-64 and Hoechst fluorescence signals in protoplasts cell membrane and nucleus, respectively (Figures 3b and S6). Orthogonal projections from Z-stacks of different planes (x/y, x/z, or y/z) of the confocal microscope images confirmed nuclear uptake of GT_{15}-Cy3 using TMGMV-PAH as shown by the colocalization with Hoechst fluorescence dye (Figure 3c). Quantitative subcellular localization analysis indicated that approximately 38% ± 1.5 of the GT_{15}-Cy3 fluorescence signal was observed in protoplast cell membranes, while 11% ± 3.0 localized with a nuclear marker (Hoechst; Figure 3d). Together, our results indicate that high aspect ratio and highly positive charged TMGMV-PAH allow penetration through plant cell membranes and facilitate ssDNA delivery (GT_{15}-Cy3) into the nucleus, similar to inorganic high aspect ratio nanomaterials with positive charge.[23]

To elucidate the mechanism of DNA delivery into plant cells by TMGMV-PAH, we conducted a cell uptake assay with TMGMV-PAH-GT_{15}-Cy3 at 4 °C to inhibit energy-dependent uptake mechanisms, including endocytosis.[53] We observed a similar percentage of protoplasts with GT_{15}-Cy3 delivery by TMGMV-PAH at 4 °C (10% ± 1.6) and 25 °C (11% ± 3.2) (Figure S7). Thus, DNA delivered by TMGMV-PAH passively traverses the protoplast membrane by an energy-independent mechanism. This is consistent with previous studies demonstrating that highly charged inorganic nanomaterials spontaneously penetrate plant cells, by creating temporary pores in their lipid membranes.[23,24,33,54,55] To determine the specific endocytosis pathways involved in nanoparticle uptake, a variety of endocytosis inhibitors can be employed.[56] However, temperature dependent assays block all endocytosis pathways, thus giving unequivocal evidence that the nanocarriers are not taken up through energy dependent mechanisms.

We investigated the TMGMV-PAH loading of pDNA, encoding a green fluorescent protein (GFP) in a transient expression vector (p35S-eGFP) (Figure S8), and delivery in *Arabidopsis* protoplasts. The TMGMV-PAH-pDNA were loaded at various concentrations of pDNA (TMGMV-PAH:pDNA mass ratios 1:1 to 1:20 w/w). The gel electrophoresis of pDNA mobility shift assay (EMSA) showed no unbound or free pDNA running into the agarose gel at a mass ratio of TMGMV-PAH/pDNA = 1:1 to 1:12 (w/w), meaning that pDNA loading was 100% up to a 1:12 (w/w) mass ratio (Figure 4a). The 1:12 TMGMV-PAH to pDNA mass loading ratio is multiple times higher than the 1:2 and 10:1 nanomaterial/pDNA loading ratio reported in previous studies using inorganic nanomaterials for DNA delivery in plant cells.[23,57] Oversaturated and unbound free pDNA bands were observed at TMGMV-PAH/pDNA mass ratios of 1:20 (w/w) and higher in EMSA (Figure 4a). The loading of pDNA gradually reduced ζ potential as the loading ratio of pDNA increased from 1:1 to 1:12 (Figure 4b) due to the electrostatic bonding between the negatively charged pDNA and the positively charged TMGMV-PAH. The highest decrease in ζ potential was observed after pDNA loading to TMGMV-PAH at a mass ratio of 1:12, dropping from the initial +57.53 ± 5.2 mV for TMGMV-PAH to +9.57 ± 10.6 mV ($P < 0.0001$; Figure 4b). At the loading mass ratio of 1:20, the ζ potential became negative, −31.17 ± 6.4 mV, representing the oversaturation of the nanocarriers and free pDNA in the suspension. This finding indicates maximum pDNA loading at a 1:12 mass ratio and is consistent with our EMSA analysis. We confirmed morphological integrity of TMGMV-PAH loaded with pDNA from 1:1 to 1:12 mass ratios by TEM (Figures 4c and S9). In addition, we also assessed pDNA stability by an *in vitro* pDNA degradation assay using DNase I (nuclease), which showed that pDNA molecules, when loaded onto TMGMV-PAH, were protected from DNase I nuclease activity (Figure S10).

To demonstrate pDNA delivery and expression in plant cells, we incubated isolated protoplasts with TMGMV-PAH-pDNA complexes at 1:6 mass ratio having a high positive charge (+42.16 ± 5.1 mV) and loading of pDNA (Figure 4b) to promote uptake through lipid membranes[49] and increase the amount of pDNA delivery, respectively. We used 25 μg of pDNA for TMGMV-PAH-mediated protoplast transformation, a standard concentration of pDNA (5−30 μg) established for PEG-mediated protoplast transformation.[58] Therefore, we

https://doi.org/10.1021/acs.nanolett.3c04735
Nano Lett. XXXX, XXX, XXX−XXX

adjusted the TMGMV-PAH concentration to 0.04 mg/mL to keep a 1:6 mass ratio of the pDNA loading. Protoplasts were incubated with TMGMV-PAH-pDNA, and gene expression was determined after 24 h by confocal fluorescence microscopy imaging. We observed GFP expression in protoplasts when incubated with TMGMV-PAH-pDNA (Figure 4d) at a 16% ± 3.0 ($P < 0.001$) transformation efficiency. This transformation efficiency is lower than what is reported for PEG-mediated transformation in *Arabidopsis* plant protoplasts (50% to 90% in viable cells).[48] However, this demonstrates that virus-like nanocarriers can be engineered to deliver DNA to the plant nuclear genome. Further optimization of plant virus type or the nanocarrier charge, size, and aspect ratio properties may result in higher transformation efficiencies. Nevertheless, GFP expression was observed using TMGMV-PAH-pDNA, but was not detected when protoplasts were incubated with pDNA alone and TMGMV-PAH alone (Figure 4d). To further confirm GFP expression in protoplasts treated with TMGMV-PAH-pDNA, we performed a Western blot analysis on total soluble protein using an anti-GFP antibody, which detected an ~27 kDa GFP-specific protein band (Figure 4e).

For GFP expression analysis *in vivo*, we inactivated TMGMV to prevent plant infection using UV light exposure as reported previously.[43] The TEM size of inactivated iTMGMV (110.73 ± 30.22 nm) is similar to those of active TMGMV (129.9 ± 57.7 nm) ($P > 0.05$) (Figure S11). In contrast, the zeta potential of iTMGMV is more negative (−36.29 ± 4.23 mV) compared to that of active TMGMV (−22.4 ± 2.3 mV) (10 mM MES Buffer, pH 6.0) ($P < 0.0001$). This resulted in iTMGMV-PAH-pDNA having a higher zeta potential (58.53 ± 0.50 mV) than TMGMV-PAH-pDNA (42.16 ± 5.1 mV; $P < 0001$). We abaxially infiltrated the inactivated iTMGMV-PAH coated in pDNA into 3-week-old *Arabidopsis* leaves at the previously established 1:6 mass loading ratio. Confocal microscopy analysis indicated that 0.1 mg/mL of iTMGMV-PAH bound to 0.6 mg/mL of pDNA can enable GFP expression into leaf epidermal cells (Figure 5a). Buffer or iTMGMV-PAH infiltrated leaves did not exhibit GFP fluorescence (Figure S12). Leaves infiltrated with iTMGMV-PAH-pDNA had a high GFP fluorescence intensity (Figure 5b). RT-qPCR analysis quantifying GFP mRNA fold change expression supported GFP expression mediated by 0.1 mg/mL iTMGMV-PAH:0.6 mg/mL pDNA (Figure 5c). Together, these analyses show that (i)TMGMV-PAHs have the highest pDNA mass loading ratio for nanocarriers reported to date, preserve and protect the pDNA integrity from degradation, and facilitate spontaneous pDNA translocation across the plant plasma membrane and cell wall, enabling transgene expression in the nucleus *in vitro* and *in vivo*.

Maintaining cell viability after exposure to nanocarriers with DNA is crucial for enabling biocompatible gene delivery tools for plants.[59] We evaluated protoplast viability of TMGMV-PAH coated with GT_{15}-Cy3 (0.1−0.5 mg/mL) or pDNA (0.04 mg/mL) using fluorescein diacetate (FDA),[60] a lipophilic fluorescent dye that is permeable to membranes of living cells. Following endogenous esterase-mediated enzymatic activity, nonfluorescent FDA is transformed to fluorescein, a green fluorescence compound. Broken cells lack esterases, rendering them devoid of fluorescein signal. The FDA-treated protoplast cells were analyzed by confocal microscopy imaging, and viable cell percentages were calculated based on the fluorescein presence. Both TMGMV-PAH-GT_{15}-Cy3 or TMGMV-PAH-pDNA treated and control (untreated) protoplasts showed bright green fluorescence characteristic of fluorescein and normal morphology (Figure S13a,b). Approximately 71% ± 3.5 of cells remained viable after exposure to TMGMV-PAH-GT_{15}-Cy3 (0.1 mg/mL), while increased concentrations resulted in a gradual reduction in fluorescein signal and increased number of broken cells (Figure S13c). A dramatic reduction in the fluorescein signal in protoplasts was observed after exposure to TMGMV-PAH-GT_{15}-Cy3 (0.5 mg/mL), in which almost no viable cells were observed (Figure S13c). For protoplasts exposed to the TMGMV-PAH:pDNA mass ratio (1:3), approximately 74% ± 3.0 of cells remained viable, which is not significantly different from the viability of untreated protoplasts (Figure S13d). In contrast, when TMGMV-PAH was loaded with pDNA at the mass ratios of 1:6 and 1:12, significant decreases were observed in cell viability, approximately 65% ± 5.5 ($P < 0.039$) at the 1:6 ratio and 43% ± 8.5 ($P < 0.0003$) at the 1:12 ratio cells were viable when compared to the protoplasts-only cells (Figure S13d). The TMGMV-PAH-pDNA concentration in this protoplast viability assay was kept similar to that used in the transformation analysis (0.04 mg/mL). These findings suggest that an increased loading of pDNA onto TMGMV-PAH can affect plant cell viability. Biocompatibility of iTMGMV-PAH-pDNA in *Arabidopsis* leaves was determined using propidium iodide, a fluorescent dye that stains the nucleus of dead cells (Figure S14). Confocal microscopy images of leaf cells infiltrated with our chosen concentration for GFP expression analysis of 0.1 mg/mL iTMGMV-PAH: 0.6 mg/mL pDNA showed a similar percentage of dead cells (4.5 ± 1.7%) to leaves treated with buffer control (7.9 ± 3.4%; $P > 0.5$; Figure S14a,b). Higher concentrations of 0.15 mg/mL iTMGMV-PAH: 0.9 mg/mL pDNA significantly increased the percentage of dead cells (15.8 ± 2.2%; $P < 0.01$). Overall, our results indicate that DNA coated TMGMV-PAH are highly biocompatible with plant cells both in vitro in plant protoplasts and in vivo in leaf cells.

We engineered plant virus coat protein nanocarriers (TMGMV-PAH) for facile plasmid DNA delivery into the plant cell nucleus without mechanical or biological aid, with high biocompatibility and the highest loading of DNA nanocarriers for plant cells reported to date. We demonstrated this approach using TMGMV-PAH that spontaneously delivered a transgene (GFP) encoded in an expression vector (pDNA) into plant protoplasts and epidermal cell nuclei. GFP gene delivery and expression in plant cells has been mediated by high aspect ratio carbon nanotubes.[23−25,33] In this work, we used high aspect ratio protein-based nanomaterials, native TMGMV in protoplasts, and inactivated iTMGMVs *in vivo* to prevent plant infection.[43] TMGMV's ability to move across plant cell barriers in numerous plant species[43,61] suggests that these nanocarriers could mediate DNA delivery to protoplasts or leaf cells from different plant species.

Future research will assess if pDNA mediated delivery by TMGMV-PAHs in plant cells results in transient expression of transgenes, similar to what has been reported in previous studies about pDNA delivery using inorganic nanomaterials.,[23,24,33] or enable stable plant transformation and genome editing with higher efficiency compared to current DNA delivery protocols using biological or mechanical aid. TMGMV may prove to be a promising tool for the delivery of genes, small-interfering RNA (siRNA), and clustered regularly interspaced short palindromic repeats (CRISPR) in plants for gene editing applications. Targeted delivery approaches

https://doi.org/10.1021/acs.nanolett.3c04735
Nano Lett. XXXX, XXX, XXX−XXX

could be implemented for TMGMV-mediated gene delivery into plastid genomes including coating with targeting peptides[62] for gene delivery to plant chloroplasts,[24,62] and mitochondria.[25] Our nanotechnology approach utilizing TMGMV-PAH for DNA delivery paves the way for developing plant virus-based nanocarriers with tunable and well-controlled properties,[41,42,63] cost-effectiveness, scalability,[64,65] degradability,[63] and high biocompatibility,[63,66] which enable more sustainable agriculture and advanced plant bioengineering.

■ ASSOCIATED CONTENT

Supporting Information

The Supporting Information is available free of charge at https://pubs.acs.org/doi/10.1021/acs.nanolett.3c04735.

Detailed experimental procedures, including nanocarrier synthesis and characterization, microscopy, protoplast isolation, abaxial infiltration, RT-qPCR, gel electrophoresis, and biocompatibility assays (PDF)

■ AUTHOR INFORMATION

Corresponding Authors

Nicole F. Steinmetz − *Department of NanoEngineering, University of California, San Diego, La Jolla, California 92093, United States; Department of Bioengineering, Department of Radiology, Center for Nano-Immuno Engineering, Shu and K.C. Chien and Peter Farrell Collaboratory, Institute for Materials Discovery and Design, Moores Cancer Center, and Center for Engineering in Cancer, Institute for Engineering in Medicine, University of California, San Diego, La Jolla, California 92093, United States;* orcid.org/0000-0002-0130-0481; Email: nsteinmetz@ucsd.edu

Juan Pablo Giraldo − *Department of Botany and Plant Sciences, University of California, Riverside, California 92507, United States;* orcid.org/0000-0002-8400-8944; Email: juanpablo.giraldo@ucr.edu

Authors

Md Reyazul Islam − *Department of Botany and Plant Sciences, University of California, Riverside, California 92507, United States;* orcid.org/0000-0001-9494-3197

Marina Anderson-Youngblood − *Department of Botany and Plant Sciences, University of California, Riverside, California 92507, United States;* orcid.org/0009-0004-9588-8168

Hye-In Kim − *Department of Botany and Plant Sciences, University of California, Riverside, California 92507, United States;* orcid.org/0000-0002-5203-7361

Ivonne González-Gamboa − *Department of NanoEngineering, University of California, San Diego, La Jolla, California 92093, United States; Department of Molecular Biology, University of California, San Diego, La Jolla, California 92093, United States;* orcid.org/0000-0003-1617-8252

Andrea Gabriela Monroy-Borrego − *Department of NanoEngineering, University of California, San Diego, La Jolla, California 92093, United States*

Adam A. Caparco − *Department of NanoEngineering, University of California, San Diego, La Jolla, California 92093, United States;* orcid.org/0000-0002-8545-8349

Gregory V. Lowry − *Department of Civil and Environmental Engineering and Center for Environmental Implications of NanoTechnology (CEINT), Carnegie Mellon University, Pittsburgh, Pennsylvania 15213, United States;* orcid.org/0000-0001-8599-008X

Complete contact information is available at: https://pubs.acs.org/10.1021/acs.nanolett.3c04735

Author Contributions

[#]These authors contributed equally to this work (M.R.I. and M.A.-Y.). J.P.G and N.F.S. conceived the idea and designed experiments with M.R.I. M.R.I performed nanomaterial synthesis and characterization, in vitro DNA loading and delivery, gene expression analysis, cell viability, endocytosis, and confocal microscopy assays. J.P.G designed *in vivo* experiments with M.A.-Y. who performed inactivated nanomaterial synthesis, *in vivo* pDNA delivery and gene expression analysis using RT-qPCR and confocal microscopy, and biocompatibility assays. N.F.S. and A.A.C. designed the iTMGMV formulation for the *in vivo* studies, which was prepared and characterized for quality control by A.A.C. G.V.L contributed with data analysis. H.K. performed polymer coating design and synthesis of nanocarriers, TEM, zeta potential, and FTIR analysis of nanomaterials. I.G.-G. purified and lyophilized native TMGMV. A.G.M.-B. performed TEM of nanomaterials loaded with plasmid DNA and analysis with I.G.-G. All authors contributed to writing the manuscript.

Notes

The authors declare the following competing financial interest(s): A pending patent entitled Compositions and Methods for Delivery of Nucleic Acids is based on this work. J.P.G., M.R.I., H.K. (University of California, Riverside), and N.F.S. (University of California, San Diego) are inventors in this patent. Specific aspects of the manuscript covered in the patent disclosure include compositions and methods for delivery of DNA in plant cells. N.F.S. is a cofounder of, has equity in, and has a financial interest in Mosaic ImmunoEngineering Inc. N.F.S. is a cofounder and serves as manager of Pokometz Scientific LLC, under which she is a paid as a consultant to Mosaic ImmunoEngineering Inc., Flagship Laboratories 95 Inc., and Arana Biosciences Inc. The other authors declare no potential conflict of interest.

■ ACKNOWLEDGMENTS

This material is based on work mainly supported by the National Science Foundation under Grant FMSG: Bio: 2134535. M.A.Y. received funding from NSF National Research Traineeship Program Grant DBI-1922642. A.G.M.-B. was supported by a CONAHCYT doctoral studies scholarship (CVU 1062156). A.A.C. was supported through NIFA-2022-67012-36698. We also thank partial support from UC San Diego Materials Research Science and Engineering Center (MRSEC) through NSF Grant DMR-2011924 to N.F.S. The authors thank the University of California San Diego - Cellular and Molecular Medicine Electron Microscopy Core (UCSD-CMM-EM Core, RRID:SCR_022039) for equipment access and technical assistance. The UCSD-CMM-EM Core is supported in part by the National Institutes of Health Award Number S10OD023527.

■ REFERENCES

(1) van Dijk, M.; Morley, T.; Rau, M. L.; Saghai, Y. A Meta-Analysis of Projected Global Food Demand and Population at Risk of Hunger for the Period 2010−2050. *Nat. Food* **2021**, *2* (7), 494−501.

(2) Intergovernmental Panel on Climate Change (IPCC). Food Security. *Climate Change and Land: IPCC Special Report on Climate Change, Desertification, Land Degradation, Sustainable Land Management, Food Security, and Greenhouse Gas Fluxes in Terrestrial Ecosystems*; Cambridge University Press, 2022; pp 437−550.
(3) Sedeek, K. E. M.; Mahas, A.; Mahfouz, M. Plant Genome Engineering for Targeted Improvement of Crop Traits. *Front. Plant Sci.* **2019**, *10*, 114.
(4) Daniell, H.; Datta, R.; Varma, S.; Gray, S.; Lee, S. B. Containment of Herbicide Resistance through Genetic Engineering of the Chloroplast Genome. *Nat. Biotechnol.* **1998**, *16* (4), 345−348.
(5) Liu, Y.; Wu, H.; Chen, H.; Liu, Y.; He, J.; Kang, H.; Sun, Z.; Pan, G.; Wang, Q.; Hu, J.; Zhou, F.; Zhou, K.; Zheng, X.; Ren, Y.; Chen, L.; Wang, Y.; Zhao, Z.; Lin, Q.; Wu, F.; Zhang, X.; Guo, X.; Cheng, X.; Jiang, L.; Wu, C.; Wang, H.; Wan, J. A Gene Cluster Encoding Lectin Receptor Kinases Confers Broad-Spectrum and Durable Insect Resistance in Rice. *Nat. Biotechnol.* **2015**, *33* (3), 301−305.
(6) van Esse, H. P.; Reuber, T. L.; van der Does, D. Genetic Modification to Improve Disease Resistance in Crops. *New Phytol.* **2020**, *225* (1), 70−86.
(7) Liu, X.; Ao, K.; Yao, J.; Zhang, Y.; Li, X. Engineering Plant Disease Resistance against Biotrophic Pathogens. *Curr. Opin. Plant Biol.* **2021**, *60*, No. 101987.
(8) Zhang, H.; Zhu, J.; Gong, Z.; Zhu, J.-K. Abiotic Stress Responses in Plants. *Nat. Rev. Genet.* **2022**, *23* (2), 104−119.
(9) Saijo, Y.; Loo, E. P.-I. Plant Immunity in Signal Integration between Biotic and Abiotic Stress Responses. *New Phytol.* **2020**, *225* (1), 87−104.
(10) Srivastav, V. K.; Egbuna, C.; Tiwari, M. Chapter 1 - Plant Secondary Metabolites as Lead Compounds for the Production of Potent Drugs. In *Phytochemicals as Lead Compounds for New Drug Discovery*; Egbuna, C., Kumar, S., Ifemeje, J. C., Ezzat, S. M., Kaliyaperumal, S., Eds.; Elsevier, 2020; pp 3−14.
(11) Wolfson, W. Grow Your Own: Protalix BioTherapeutics Produces Drugs in Carrot Cells. *Chem. Biol.* **2013**, *20* (8), 969−970.
(12) Daniell, H.; Nair, S. K.; Esmaeili, N.; Wakade, G.; Shahid, N.; Ganesan, P. K.; Islam, M. R.; Shepley-McTaggart, A.; Feng, S.; Gary, E. N.; Ali, A. R.; Nuth, M.; Cruz, S. N.; Graham-Wooten, J.; Streatfield, S. J.; Montoya-Lopez, R.; Kaznica, P.; Mawson, M.; Green, B. J.; Ricciardi, R.; Milone, M.; Harty, R. N.; Wang, P.; Weiner, D. B.; Margulies, K. B.; Collman, R. G. Debulking SARS-CoV-2 in Saliva Using Angiotensin Converting Enzyme 2 in Chewing Gum to Decrease Oral Virus Transmission and Infection. *Mol. Ther.* **2022**, *30* (5), 1966−1978.
(13) Paolino, K. M.; Regules, J. A.; Moon, J. E.; Ruck, R. C.; Bennett, J. W.; Remich, S. A.; Mills, K. T.; Lin, L.; Washington, C. N.; Fornillos, G. A.; Lindsey, C. Y.; O'Brien, K. A.; Shi, M.; Mark Jones, R.; Green, B. J.; Tottey, S.; Chichester, J. A.; Streatfield, S. J.; Yusibov, V. Safety and Immunogenicity of a Plant-Derived Recombinant Protective Antigen (rPA)-Based Vaccine against Bacillus Anthracis: A Phase 1 Dose-Escalation Study in Healthy Adults. *Vaccine* **2022**, *40* (12), 1864−1871.
(14) Charland, N.; Gobeil, P.; Pillet, S.; Boulay, I.; Séguin, A.; Makarkov, A.; Heizer, G.; Bhutada, K.; Mahmood, A.; Trépanier, S.; Hager, K.; Jiang-Wright, J.; Atkins, J.; Saxena, P.; Cheng, M. P.; Vinh, D. C.; Boutet, P.; Roman, F.; Van Der Most, R.; Ceregido, M. A.; Dionne, M.; Tellier, G.; Gauthier, J.-S.; Essink, B.; Libman, M.; Haffizulla, J.; Fréchette, A.; D'Aoust, M.-A.; Landry, N.; Ward, B. J. Safety and Immunogenicity of an AS03-Adjuvanted Plant-Based SARS-CoV-2 Vaccine in Adults with and without Comorbidities. *NPJ. Vaccines* **2022**, *7* (1), 142.
(15) Herrera-Estrella, L.; Depicker, A.; Van Montagu, M.; Schell, J. Expression of Chimaeric Genes Transferred into Plant Cells Using a Ti-Plasmid-Derived Vector. *Nature* **1983**, *303* (5914), 209.
(16) Klein, T. M.; Harper, E. C.; Svab, Z.; Sanford, J. C.; Fromm, M. E.; Maliga, P. Stable Genetic Transformation of Intact Nicotiana Cells by the Particle Bombardment Process. *Proc. Natl. Acad. Sci. U. S. A.* **1988**, *85* (22), 8502−8505.
(17) Shrawat, A. K.; Lörz, H. Agrobacterium-Mediated Transformation of Cereals: A Promising Approach Crossing Barriers. *Plant Biotechnol. J.* **2006**, *4* (6), 575−603.
(18) Ye, X.; Shrawat, A.; Moeller, L.; Rode, R.; Rivlin, A.; Kelm, D.; Martinell, B. J.; Williams, E. J.; Paisley, A.; Duncan, D. R.; Armstrong, C. L. Agrobacterium-Mediated Direct Transformation of Wheat Mature Embryos through Organogenesis. *Front. Plant Sci.* **2023**, *14*, No. 1202235.
(19) Hayta, S.; Smedley, M. A.; Clarke, M.; Forner, M.; Harwood, W. A. An Efficient Agrobacterium-Mediated Transformation Protocol for Hexaploid and Tetraploid Wheat. *Curr. Protoc* **2021**, *1* (3), No. e58.
(20) Liu, J.; Nannas, N. J.; Fu, F.-F.; Shi, J.; Aspinwall, B.; Parrott, W. A.; Dawe, R. K. Genome-Scale Sequence Disruption Following Biolistic Transformation in Rice and Maize. *Plant Cell* **2019**, *31* (2), 368−383.
(21) Frame, B. R.; Zhang, H.; Cocciolone, S. M.; Sidorenko, L. V.; Dietrich, C. R.; Pegg, S. E.; Zhen, S.; Schnable, P. S.; Wang, K. Production of Transgenic Maize from Bombarded Type II Callus: Effect of Gold Particle Size and Callus Morphology on Transformation Efficiency. *In Vitro Cellular & Developmental Biology - Plant* **2000**, *36* (1), 21−29.
(22) Baltes, N. J.; Gil-Humanes, J.; Voytas, D. F. Genome Engineering and Agriculture: Opportunities and Challenges. *Prog. Mol. Biol. Transl. Sci.* **2017**, *149*, 1−26.
(23) Demirer, G. S.; Zhang, H.; Matos, J. L.; Goh, N. S.; Cunningham, F. J.; Sung, Y.; Chang, R.; Aditham, A. J.; Chio, L.; Cho, M.-J.; Staskawicz, B.; Landry, M. P. High Aspect Ratio Nanomaterials Enable Delivery of Functional Genetic Material without DNA Integration in Mature Plants. *Nat. Nanotechnol.* **2019**, *14* (5), 456−464.
(24) Santana, I.; Jeon, S.-J.; Kim, H.-I.; Islam, M. R.; Castillo, C.; Garcia, G. F. H.; Newkirk, G. M.; Giraldo, J. P. Targeted Carbon Nanostructures for Chemical and Gene Delivery to Plant Chloroplasts. *ACS Nano* **2022**, *16* (8), 12156−12173.
(25) Law, S. S. Y.; Liou, G.; Nagai, Y.; Giménez-Dejoz, J.; Tateishi, A.; Tsuchiya, K.; Kodama, Y.; Fujigaya, T.; Numata, K. Polymer-Coated Carbon Nanotube Hybrids with Functional Peptides for Gene Delivery into Plant Mitochondria. *Nat. Commun.* **2022**, *13* (1), 2417.
(26) Mitter, N.; Worrall, E. A.; Robinson, K. E.; Li, P.; Jain, R. G.; Taochy, C.; Fletcher, S. J.; Carroll, B. J.; Lu, G. Q. M.; Xu, Z. P. Clay Nanosheets for Topical Delivery of RNAi for Sustained Protection against Plant Viruses. *Nat. Plants* **2017**, *3*, No. 16207.
(27) Li, S.; Li, J.; Du, M.; Deng, G.; Song, Z.; Han, H. Efficient Gene Silencing in Intact Plant Cells Using siRNA Delivered By Functional Graphene Oxide Nanoparticles. *Angew. Chem., Int. Ed.* **2022**, *61* (40), No. e202210014.
(28) Wang, J. W.; Cunningham, F. J.; Goh, N. S.; Boozarpour, N. N.; Pham, M.; Landry, M. P. Nanoparticles for Protein Delivery in Planta. *Curr. Opin. Plant Biol.* **2021**, *60*, No. 102052.
(29) Chariou, P. L.; Steinmetz, N. F. Delivery of Pesticides to Plant Parasitic Nematodes Using Tobacco Mild Green Mosaic Virus as a Nanocarrier. *ACS Nano* **2017**, *11* (5), 4719−4730.
(30) Caparco, A. A.; González-Gamboa, I.; Hays, S. S.; Pokorski, J. K.; Steinmetz, N. F. Delivery of Nematicides Using TMGMV-Derived Spherical Nanoparticles. *Nano Lett.* **2023**, *23* (12), 5785−5793.
(31) Solanki, P.; Bhargava, A.; Chhipa, H.; Jain, N.; Panwar, J. Nano-Fertilizers and Their Smart Delivery System. In *Nanotechnologies in Food and Agriculture*; Rai, M., Ribeiro, C., Mattoso, L., Duran, N.,, Eds.; Springer International Publishing: Cham, 2015; pp 81−101.
(32) Borgatta, J.; Shen, Y.; Tamez, C.; Green, C.; Hedlund Orbeck, J. K.; Cahill, M. S.; Protter, C.; Deng, C.; Wang, Y.; Elmer, W.; White, J. C.; Hamers, R. J. Influence of CuO Nanoparticle Aspect Ratio and Surface Charge on Disease Suppression in Tomato (Solanum Lycopersicum). *J. Agric. Food Chem.* **2023**, *71*, 9644.
(33) Kwak, S.-Y.; Lew, T. T. S.; Sweeney, C. J.; Koman, V. B.; Wong, M. H.; Bohmert-Tatarev, K.; Snell, K. D.; Seo, J. S.; Chua, N.-H.; Strano, M. S. Chloroplast-Selective Gene Delivery and Expression in

https://doi.org/10.1021/acs.nanolett.3c04735
Nano Lett. XXXX, XXX, XXX−XXX

Planta Using Chitosan-Complexed Single-Walled Carbon Nanotube Carriers. *Nat. Nanotechnol.* **2019**, *14* (5), 447−455.
(34) Chang, F.-P.; Kuang, L.-Y.; Huang, C.-A.; Jane, W.-N.; Hung, Y.; Hsing, Y.-I. C.; Mou, C.-Y. A Simple Plant Gene Delivery System Using Mesoporous Silica Nanoparticles as Carriers. *J. Mater. Chem. B Mater. Biol. Med.* **2013**, *1* (39), 5279−5287.
(35) Torney, F.; Trewyn, B. G.; Lin, V. S.-Y.; Wang, K. Mesoporous Silica Nanoparticles Deliver DNA and Chemicals into Plants. *Nat. Nanotechnol.* **2007**, *2* (5), 295−300.
(36) Li, J.; Li, S.; Du, M.; Song, Z.; Han, H. Nuclear Delivery of Exogenous Gene in Mature Plants Using Nuclear Location Signal and Cell-Penetrating Peptide Nanocomplex. *ACS Appl. Nano Mater.* **2023**, *6* (1), 160−170.
(37) Jones, I.; Roy, P. Small Is Beautiful: Virus-like Particles as Vaccines. *Biochem.* **2021**, *43* (4), 18−21.
(38) Pattanayek, R.; Stubbs, G. Structure of the U2 Strain of Tobacco Mosaic Virus Refined at 3.5 A Resolution Using X-Ray Fiber Diffraction. *J. Mol. Biol.* **1992**, *228* (2), 516−528.
(39) Charudattan, R. Use of Plant Viruses as Bioherbicides: The First Virus-Based Bioherbicide and Future Opportunities. *Pest Manag. Sci.* **2024**, *80*, 103.
(40) Chariou, P. L.; Wang, L.; Desai, C.; Park, J.; Robbins, L. K.; von Recum, H. A.; Ghiladi, R. A.; Steinmetz, N. F. Let There Be Light: Targeted Photodynamic Therapy Using High Aspect Ratio Plant Viral Nanoparticles. *Macromol. Biosci.* **2019**, *19* (5), No. e1800407.
(41) Fan, X. Z.; Pomerantseva, E.; Gnerlich, M.; Brown, A.; Gerasopoulos, K.; McCarthy, M.; Culver, J.; Ghodssi, R. Tobacco Mosaic Virus: A Biological Building Block for Micro/nano/bio Systems. *J. Vac. Sci. Technol. A* **2013**, *31* (5), No. 050815.
(42) González-Gamboa, I.; Caparco, A. A.; McCaskill, J. M.; Steinmetz, N. F. Bioconjugation Strategies for Tobacco Mild Green Mosaic Virus. *ChemBioChem* **2022**, *23* (18), No. e202200323.
(43) Chariou, P. L.; Ma, Y.; Hensley, M.; Rosskopf, E. N.; Hong, J. C.; Charudattan, R.; Steinmetz, N. F. Inactivated Plant Viruses as an Agrochemical Delivery Platform. *ACS Agric. Sci. Technol.* **2021**, *1* (3), 124−130.
(44) González-Gamboa, I.; Caparco, A. A.; McCaskill, J.; Fuenlabrada-Velázquez, P.; Hays, S. S.; Jin, Z.; Jokerst, J. V.; Pokorski, J. K.; Steinmetz, N. F. Inter-Coat Protein Loading of Active Ingredients into Tobacco Mild Green Mosaic Virus through Partial Dissociation and Reassembly of the Virion. *Sci. Rep.* **2024**, *14* (1), 7168.
(45) Abrahamian, P.; Hammond, R. W.; Hammond, J. Plant Virus-Derived Vectors: Applications in Agricultural and Medical Biotechnology. *Annu. Rev. Virol* **2020**, *7* (1), 513−535.
(46) Scholthof, K.-B. G.; Mirkov, T. E.; Scholthof, H. B. Plant Virus Gene Vectors: Biotechnology Applications in Agriculture and Medicine. *Genet. Eng.* **2002**, *24*, 67−85.
(47) Rössner, C.; Lotz, D.; Becker, A. VIGS Goes Viral: How VIGS Transforms Our Understanding of Plant Science. *Annu. Rev. Plant Biol.* **2022**, *73*, 703−728.
(48) Yoo, S.-D.; Cho, Y.-H.; Sheen, J. Arabidopsis Mesophyll Protoplasts: A Versatile Cell System for Transient Gene Expression Analysis. *Nat. Protoc.* **2007**, *2* (7), 1565−1572.
(49) Lew, T. T. S.; Wong, M. H.; Kwak, S.-Y.; Sinclair, R.; Koman, V. B.; Strano, M. S. Rational Design Principles for the Transport and Subcellular Distribution of Nanomaterials into Plant Protoplasts. *Small* **2018**, *14* (44), No. e1802086.
(50) Jian, W.; Xu, S.; Wang, J.; Feng, S. Layer-by-Layer Assembly of Poly(allylamine Hydrochloride)/polyurethane and Its Loading and Release Behavior for Methylene Orange. *J. Appl. Polym. Sci.* **2013**, *129* (4), 2070−2075.
(51) Kreke, M. R.; Badami, A. S.; Brady, J. B.; Akers, R. M.; Goldstein, A. S. Modulation of Protein Adsorption and Cell Adhesion by Poly(allylamine hydrochloride) Heparin Films. *Biomaterials* **2005**, *26* (16), 2975−2981.
(52) Giraldo, J. P.; Landry, M. P.; Kwak, S.-Y.; Jain, R. M.; Wong, M. H.; Iverson, N. M.; Ben-Naim, M.; Strano, M. S. A Ratiometric Sensor Using Single Chirality Near-Infrared Fluorescent Carbon Nanotubes: Application to In Vivo Monitoring. *Small* **2015**, *11* (32), 3973−3984.
(53) He, Z.; Liu, K.; Manaloto, E.; Casey, A.; Cribaro, G. P.; Byrne, H. J.; Tian, F.; Barcia, C.; Conway, G. E.; Cullen, P. J.; Curtin, J. F. Cold Atmospheric Plasma Induces ATP-Dependent Endocytosis of Nanoparticles and Synergistic U373MG Cancer Cell Death. *Sci. Rep.* **2018**, *8* (1), 5298.
(54) Giraldo, J. P.; Landry, M. P.; Faltermeier, S. M.; McNicholas, T. P.; Iverson, N. M.; Boghossian, A. A.; Reuel, N. F.; Hilmer, A. J.; Sen, F.; Brew, J. A.; Strano, M. S. Plant Nanobionics Approach to Augment Photosynthesis and Biochemical Sensing. *Nat. Mater.* **2014**, *13* (4), 400−408.
(55) Wong, M. H.; Misra, R. P.; Giraldo, J. P.; Kwak, S.-Y.; Son, Y.; Landry, M. P.; Swan, J. W.; Blankschtein, D.; Strano, M. S. Lipid Exchange Envelope Penetration (LEEP) of Nanoparticles for Plant Engineering: A Universal Localization Mechanism. *Nano Lett.* **2016**, *16* (2), 1161−1172.
(56) Rennick, J. J.; Johnston, A. P. R.; Parton, R. G. Key Principles and Methods for Studying the Endocytosis of Biological and Nanoparticle Therapeutics. *Nat. Nanotechnol.* **2021**, *16* (3), 266−276.
(57) Liu, Q.; Li, Y.; Xu, K.; Li, D.; Hu, H.; Zhou, F.; Song, P.; Yu, Y.; Wei, Q.; Liu, Q.; Wang, W.; Bu, R.; Sun, H.; Wang, X.; Hao, J.; Li, H.; Li, C. Clay Nanosheet-Mediated Delivery of Recombinant Plasmids Expressing Artificial miRNAs via Leaf Spray to Prevent Infection by Plant DNA Viruses. *Hortic Res.* **2020**, *7* (1), 179.
(58) Lee, D. W.; Hwang, I. Transient Expression and Analysis of Chloroplast Proteins in Arabidopsis Protoplasts. In *Chloroplast Research in Arabidopsis: Methods and Protocols*; Jarvis, R. P., Ed.; Humana Press: Totowa, NJ, 2011; Vol. *I*, pp 59−71.
(59) Wang, X.; Xie, H.; Wang, P.; Yin, H. Nanoparticles in Plants: Uptake, Transport and Physiological Activity in Leaf and Root. *Materials* **2023**, *16* (8), 3097.
(60) Wang, H.; Zhu, X.; Li, H.; Cui, J.; Liu, C.; Chen, X.; Zhang, W. Induction of Caspase-3-like Activity in Rice Following Release of Cytochrome-F from the Chloroplast and Subsequent Interaction with the Ubiquitin-Proteasome System. *Sci. Rep.* **2014**, *4*, 5989.
(61) de Andrés-Torán, R.; Guidoum, L.; Zamfir, A. D.; Mora, M. Á.; Moreno-Vázquez, S.; García-Arenal, F. Tobacco Mild Green Mosaic Virus (TMGMV) Isolates from Different Plant Families Show No Evidence of Differential Adaptation to Their Host of Origin. *Viruses* **2023**, *15* (12), 2384.
(62) Santana, I.; Wu, H.; Hu, P.; Giraldo, J. P. Targeted Delivery of Nanomaterials with Chemical Cargoes in Plants Enabled by a Biorecognition Motif. *Nat. Commun.* **2020**, *11* (1), 2045.
(63) Koudelka, K. J.; Pitek, A. S.; Manchester, M.; Steinmetz, N. F. Virus-Based Nanoparticles as Versatile Nanomachines. *Annu. Rev. Virol* **2015**, *2* (1), 379−401.
(64) Chung, Y. H.; Church, D.; Koellhoffer, E. C.; Osota, E.; Shukla, S.; Rybicki, E. P.; Pokorski, J. K.; Steinmetz, N. F. Integrating Plant Molecular Farming and Materials Research for next-Generation Vaccines. *Nat. Rev. Mater.* **2022**, *7* (5), 372−388.
(65) Rybicki, E. P. Plant Molecular Farming of Virus-like Nanoparticles as Vaccines and Reagents. *Wiley Interdiscip. Rev. Nanomed. Nanobiotechnol.* **2020**, *12* (2), No. e1587.
(66) Kim, K. R.; Lee, A. S.; Kim, S. M.; Heo, H. R.; Kim, C. S. Virus-like Nanoparticles as a Theranostic Platform for Cancer. *Front Bioeng Biotechnol* **2023**, *10*, No. 1106767.

https://doi.org/10.1021/acs.nanolett.3c04735
Nano Lett. XXXX, XXX, XXX−XXX